

ELECTRONIC SUPPORTING INFORMATION

ESI-MS reveals preferential complex formation of carbohydrates with *Z*- sinapinic acid compared with the *E*-isomer.

Tobías Schmidt De León,^{a,b} María Laura Salum,^{a,b} Yasuyuki Matsushita,^c Kazuhiko Fukushima,³ María Eugenia Monge^{d*} and Rosa Erra-Balsells^{a,b*}

^a Universidad de Buenos Aires. Facultad de Ciencias Exactas y Naturales. Departamento de Química Orgánica. Pabellón II, 3er P., Ciudad Universitaria, 1428 Buenos Aires, Argentina.

^b CONICET, Universidad de Buenos Aires. Centro de Investigación en Hidratos de Carbono (CIHIDECAR). Facultad de Ciencias Exactas y Naturales Pabellón II, 3er P. Ciudad Universitaria, 1428 Buenos Aires, Argentina.

^c Laboratory of Forest Chemistry, Department of Forest and Environmental Resources Sciences, Graduate school of Bioagricultural Sciences, Nagoya University, Furo-cho, Chikusa-ku, Nagoya 464-0814, Japan.

^d Centro de Investigaciones en Bionanociencias (CIBION), Consejo Nacional de Investigaciones Científicas y Técnicas (CONICET), Godoy Cruz 2390, C1425FQD, Ciudad de Buenos Aires, Argentina.

Corresponding authors:

Rosa Erra-Balsells. Fax/Phone: +54-1152858532 (ext. 58532). E-mail: erra@qo.fcen.uba.ar. ORCID: <https://orcid.org/0000-0003-0169-0173>

María Eugenia Monge. Phone: +54-1148995500 (ext. 5614), E-mail: maria.monge@cibion.conicet.gov.ar. ORCID: <https://orcid.org/0000-0001-6517-5301>

TABLE of CONTENTS

E-3,5-di(methoxy-d3)-4-hydroxycinnamic acid preparation.	S-3
Molecular Modeling.	S-4
Table S1. Molecular modeling. HOMO energy and QSAR properties for ESA and ZSA	S-6
Table S2. Molecular modeling. HOMO energy and QSAR properties for carbohydrates studied.	S-7
Scheme S1. (A) Additional details for Scheme 2 (c) included in main text: (left) ESA+Glc 1:1 complex. Glc in green except the two H atoms involved in the H bridges between ESA and Glc; (right) enhances view of the H bridges interaction region. (B) Optimized molecule geometry comparison for Glc (left) and Frc (right). Molecule views from two different planes (upper row, view from ceiling plane; bottom row, view from plane perpendicular to ceiling). (C) Optimized molecule geometry comparison for β CD and M7. (a) β CD (left) and M7 (right); (b) M7 (top) and β CD (bottom); (c) idem (b) with M7 in green. (D) Optimized molecule geometry comparison for F5 and M5: (a) Artificial on silico superposition of molecules F5 (sticks and ball) and M5 (sticks); (b) Artificial on silico superposition of molecules F5 (sticks and ball) and M5 (sticks and balls in green); (c) M5 (top) and F5 (bottom) and (d) M5 (top) and F5, M5 in green.	S-8
Scheme S2. Optimized molecule geometry comparison for $[ZSA-H]^-$ and $[ESA-H]^-$.	S-11
Scheme S3. Optimized molecule geometry comparison for proposed complexes with β CD, $[ESA+\beta CD-H]^-$ and $[ZSA+\beta CD-H]^-$.	S-12
Scheme S4. Optimized molecule geometry comparison for F5 and $[F5-H]^-$.	S-13
Figure S1. Intensity of the $[Carb-H]^-$ peak relative to $[ESA-H]^-$, ($[Carb-H]^- / [ESA-H]^-$), and (b) absolute intensity of $[Carb-H]^-$ peak for each Carb.	S-14
Figure S2. Intensity of the $[ZSA+Carb-H]^-$ peak relative to $[ESA+Carb-H]^-$, ($[ZSA+Carb-H]^- / [ESA+Carb-H]^-$), for different Acid:Carb molar ratios.	S-15
Figure S3. Competitive titration curves for Carb M6.	S-16
Figure S4. MS/MS spectra. Precursor ions: $[ESA+M7-H]^-$, $[ZSA+M7-H]^-$ and $[ESA-d6-H]^-$.	S-17
Figure S5. MS/MS spectra. Precursor ions: $[ESA+M5-H]^-$, $[ZSA+M5-H]^-$ and $[ESA-d6+M5-H]^-$.	S-18
Figure S6. MS/MS spectra. Precursor ions: $[ESA+F5-H]^-$, $[ZSA+F5-H]^-$ and $[ESA-d6+F5-H]^-$.	S-19
Figure S7. MS/MS (CID) experiments. Intensity of $[Acid+M7-H]^-$. $[Acid-H]^-$ and $[M7-H]^-$ detected at different voltages.	S-20
Figure S8. MS/MS (CID) experiments. Intensity of $[Acid+Carb-H]^-$. $[Acid-H]^-$ and $[Carb-H]^-$ detected at different voltages. Carb: M5 and F5.	S-20
Figure S9. MS/MS (CID) experiments. Intensity of $[Acid+Carb-H]^-$ detected at different voltages. Carb: Glc and Frc.	S-21
Figure S10. MS/MS (CID) experiments. Intensity of $[Acid+Carb-H]^-$. $[Acid-H]^-$ and $[Carb-H]^-$ detected at different voltages. Carb: Glc and Frc.	S-21

E-3,5-di(methoxy-d3)-4-hydroxycinnamic acid preparation.

The synthesis of deuterium labeled *trans*-sinapinic acid E-3,5-di(methoxy-d3)-4-hydroxycinnamic acid (ESA-d6) was based on the method described by Yamauchi *et al.*^{1,2} After methanol-d4 (3 mL) was placed in the flask, sodium (276 mg) was added and dissolved. 3,5-Dibromo-4-hydroxybenzaldehyde (336 mg) and 1-methyl imidazole (1.5 mL) were added to the solution. After heating the mixture at 130 °C for 5 min without cap to evaporate excess of methanol-d4, copper (II) chloride (113 mg) was added and connected to a Dimroth condenser. The reaction was continued for 1 h and then cooled down to room temperature. The reaction mixture was acidified to pH=3 using hydrochloric acid, and subsequently extracted with ethyl acetate. The organic layer was washed with brine (salt saturated aqueous solution) and dried with anhydrous sodium sulfate. The solvent was removed at reduced pressure to obtain 3,5-di(methoxy-d3)-4-hydroxybenzaldehyde (318 mg, yield 82 %). This 3,5-di(methoxy-d3)aldehyde (200 mg) was condensed with malonic acid (133 mg) in pyridine (1 mL) with small amount of piperidine (1 drop) at 70°C for 5 h. The reaction mixture was acidified to pH=3 with hydrochloric acid, and subsequently extracted with ethyl acetate. The organic layer was washed with brine, and dried with anhydrous sodium sulfate. The solvent was removed at reduced pressure and the reaction product was purified by recrystallization using acetone and hexane to obtain ESA-d6 (105 mg, yield 46 %). Melting point = 185.5 °C. ¹H-NMR (500 MHz; acetone-d6; tetramethylsilane (TMS) as internal standard: chemical shift values reported in ppm; coupling constants (*J*) given in Hertz) δ (ppm): 6.40 (d, *J* = 15.9 Hz, 1H, HC α), 7.01 (s, 2H, HC(2) and HC(6)) and 7.58 (d, *J* = 15.8 Hz, 1H, HC β). High resolution MS (HRMS) data were acquired in negative ion mode: calculated *m/z* value for [M-H]⁻ with M = C₁₁H₆D₆O₅ : 229.0989; experimental *m/z*: 229.0999; HRMS/MS data were acquired in negative ion mode (CID, voltage: 15 V): precursor ion with *m/z* 229.0999 (25%), product ions with *m/z* 211.0575 (100%), *m/z* 193.0148 (27%), *m/z* 185.1070 (12%), *m/z* 150.0312 (39%), *m/z* 149.0244 (23%), *m/z* 137.0552 (4%), *m/z* 121.0275 (2%), and *m/z* 93.0331 (1%).

(1) K. Yamauchi, S. Yasuda, and K. Fukushima, *J. Agric. Food Chem.*, 2002, **50**, 3222.

(2) K. Yamauchi, S. Yasuda, K. Hamada, Y. Tsutsumi and K. Fukushima, *Planta*, 2003, **216**, 496.

Molecular Modeling.

The ground state geometry of ZSA, [ZSA-H]⁻, ESA, [ESA-H]⁻, Glc, [Glc-H]⁻, Frc, [Frc-H]⁻, F5, [F5-H]⁻, M5, [M5-H]⁻, M6, [M6-H]⁻, M7, [M7-H]⁻, βCD and [βCD-H]⁻, including three 3,5,dimethoxy-rotamers for each acid isomer and several [carbohydrate-H]⁻ isomers for each carbohydrate with different location of the deprotonated hydroxyl (O⁻C) moiety were fully optimized without imposing any symmetry constraints by *ab initio* and semiempirical methods. For *ab initio* DFT calculations, we used the hybrid gradient-corrected exchange functional combined with the gradient-corrected correlation functional, commonly known as B3LYP, which has been shown to be quite reliable for geometries. The standardized 6-311G(d,p) basis set was used for geometry optimization. We denote our B3LYP calculations by B3LYP/6-311G(d,p). For single point calculations the standardized 6-311++G(d,p) basis set was used at B3LYP theory level (B3LYP/6-311++G(d,p)//B3LYP/6-311G(d,p)). All the *ab initio* calculations were carried out using Gaussian 09.^{3,4}

The quantitative structure–activity relationship (QSAR) properties (Tables S1 and S2) and molecular orbitals (highest occupied molecular orbital (HOMO) and lowest unoccupied molecular orbital (LUMO), Tables S1 and S2) were obtained with the package implemented in the HyperChem program, after conducting a single point calculation on a geometry optimized molecule structure, by using the semiempirical parametrized PM3 method as implemented in HyperChem version 8.0.10 for Windows^{5,6} (Restricted Hartree-Fock (RHF) formalism; total charge: 0 and -1 for neutral and anionic species, respectively; multiplicity: 1; convergence limit: 1e-008; iteration limit: 50; accelerate convergence: on; CI method: none; Polak-Ribiere algorithm; RMS gradient: 0.006 kcal/(Å mol); in vacuo).

The ground-state geometry of dimeric structures (i.e., Scheme 2c-d) were calculated by using the semiempirical parametrized PM3 method as implemented in HyperChem version 8.08 for Windows^{5,6} (RHF formalism; total charge: 0; spin multiplicity: 1; convergence limit: 1e-008; iteration limit: 50; accelerate convergence: on; CI method: none; Polak-Ribiere algorithm; RMS gradient: 0.006 kcal/(Å mol); in vacuo).

(3) M.L. Salum, S.L. Giudicessi, T. Schmidt De León, S.A. Camperi and R. Erra-Balsells, *J Mass Spectrom.*, 2017, **52**, 182.

(4) Gaussian 09, Revision A.02, M.J. Frisch, G.W. Trucks, H.B. Schlegel, G.E. Scuseria, M.A. Robb, J.R. Cheeseman, G. Scalmani, V. Barone, B. Mennucci, G.A. Petersson, H. Nakatsuji, M. Caricato, X. Li, H.P. Hratchian, A.F. Izmaylov, J. Bloino, G. Zheng, J.L. Sonnenberg, M. Hada, M. Ehara, K. Toyota, R. Fukuda, J. Hasegawa, M. Ishida, T. Nakajima, Y. Honda, O. Kitao, H. Nakai, T. Vreven, J.A. Montgomery, Jr., J.E. Peralta, F. Ogliaro, M. Bearpark, J.J. Heyd, E. Brothers, K.N. Kudin, V.N. Staroverov, R. Kobayashi, J. Normand, K. Raghavachari, A. Rendell, J.C. Burant, S.S. Iyengar, J. Tomasi, M. Cossi, N. Rega, J.M. Millam, M. Klene, J.E. Knox, J.B. Cross, V. Bakken, C. Adamo, J. Jaramillo, R. Gomperts, R.E. Stratmann, O. Yazyev, A.J. Austin, R. Cammi, C. Pomelli, J.W. Ochterski, R.L. Martin, K. Morokuma, V.G. Zakrzewski, G.A. Voth, P. Salvador, J.J. Dannenberg, S. Dapprich, A.D. Daniels, O. Farkas, J.B. Foresman, J.V. Ortiz, J. Cioslowski, and D.J. Fox, Gaussian, Inc., Wallingford CT, 2009.

(5) M.L. Salum, L.M. Itovich and R. Erra-Balsells, *J. Mass Spectrom.*, 2013, **48**, 1160.

(6) HyperChem 8.0.10 for Windows, HyperCube Inc., Ontario, 2010.

Table S1. Molecular modeling. HOMO and LUMO energy and QSAR properties for ESA and ZSA

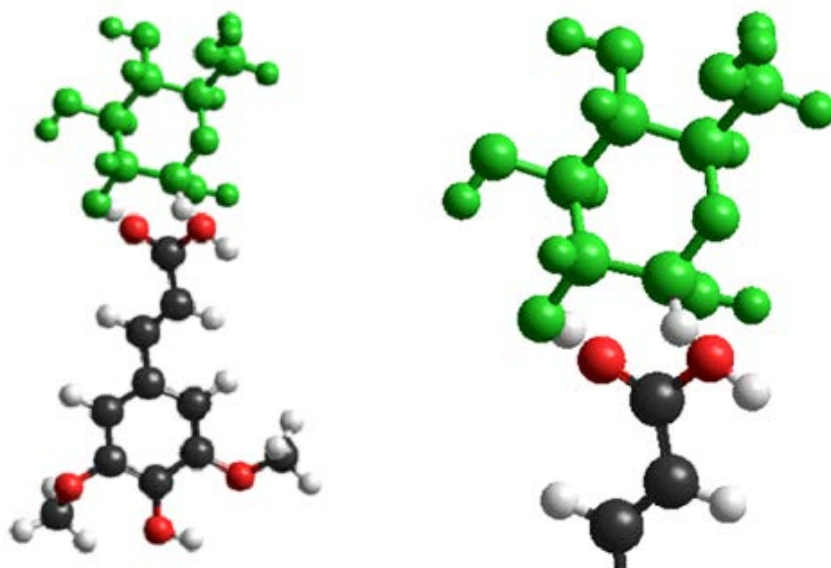
	Compound	HOMO Energy (eV)	LUMO Energy (eV)	Δ^* Energy (eV)	Dipolar moment (Debye)	Hydration Energy (kcal/mol)	LogP	Surface area (aprox.) (\AA^2)	Surface area (Grid) (\AA^2)	Volume (\AA^3)	Polarizability (\AA^3)
1	ESA	-9.245	-1.015	8.230	5.2	-15.9	-1.6	411.2	421.9	669.4	22.1
2	ESAp**	-8.891	-0.862	8.029	2.4	-13.7	-1.6	402.9	421.2	664.2	22.1
3	ESApS***	-8.795	-0.887	7.908	0.9	-14.3	-1.6	409.5	421.6	665.7	22.1
4	[ESA-H]	-4.548	2.484	7.032	20.0	-8.9	-0.2	409.7	416.8	660.8	21.6
5	[ESAp-H]**	-4.519	2.640	7.159	20.7	-8.4	-0.2	404.2	415.9	655.2	21.6
6	[ESApS-H]***	-4.555	2.653	7.208	18.5	-8.9	-0.2	410.7	417.9	656.7	21.6
7	ZSA	-9.095	-0.601	8.494	1.9	-12.8	-1.6	371.8	410.3	657.5	22.1
8	ZSAp**	-8.961	-0.560	8.401	2.6	-12.5	-1.6	368.1	412.6	654.3	22.1
9	ZSApS***	-8.773	-0.527	8.246	1.9	-12.7	-1.6	369.9	409.7	651.8	22.1
10	[ZSA-H]	-5.097	3.100	8.197	12.2	-9.9	-0.2	375.6	406.7	643.9	21.6
11	[ZSAp-H]**	-4.983	3.123	8.106	11.2	-10.0	-0.2	374.7	404.5	644.6	21.6
12	[ZSApS-H]***	-4.936	3.155	8.091	11.7	-10.1	-0.2	376.5	408.7	643.7	21.6

* $\Delta = [\text{LUMO-HOMO}]$; **p, planar structure: both O-CH₃ bond in the same plane than aromatic ring. *** ps, planar structure and symmetric position of the CH₃O-substituents, symmetry element perpendicular to the aromatic ring plane.

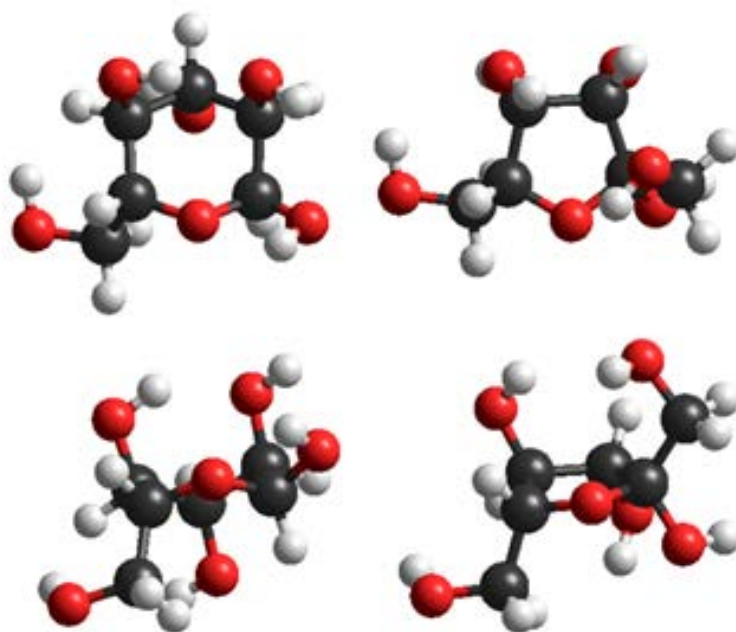
Table S2. Molecular modeling. HOMO and LUMO energy and QSAR properties for carbohydrates studied.

	Compound	HOMO Energy (eV)	LUMO Energy (eV)	Δ^* Energy (eV)	Dipolar moment (Debye)	Hydration Energy (kcal/mol)	LogP	Surface area (aprox.) (\AA^2)	Surface area (Grid) (\AA^2)	Volume (\AA^3)	Polarizability (\AA^3)
1	Glu	-10.602	2.084	12.686	1.5	-22.4	-1.8	235.7	318.7	489.9	14.8
2	Fruc	-10.930	1.862	12.792	1.5	-23.2	-1.8	267.9	325.1	504.8	14.8
4	M5	-10.390	1.271	11.661	10.3	-69.5	-6.6	794.4	1021.5	1914.6	68.5
3	F5	-10.822	1.050	11.872	3.5	-62.9	-4.6	705.1	905.5	1801.5	68.5
5	M6	-10.423	1.239	11.662	11.2	-81.1	-7.8	923.9	1203.9	2268.6	81.9
6	M7	-10.264	1.374	11.638	10.2	-93.9	-9.1	1083.4	1379.9	2636.3	95.4
7	β CD	-10.604	1.362	11.966	5.6	-76.8	-8.5	907.7	1175.2	2423.3	93.9
8	[Glu-H]										
	GluA2**	-4.252	6.401	10.653	6.4	-20.5	<0.1	238.4	312.1	475.9	14.4
	GluA3**	-3.485	6.383	9.868	5.9	-20.3		240.2	313.6	480.2	
	GluA4**	-4.044	6.462	10.506	4.8	-21.4		242.4	312.8	476.0	
	GluA6**	-3.748	6.310	10.058	6.9	-19.9		225.9	308.9	474.4	
9	[Fruc-H]										
	FrucA1**	-3.814	6.206	10.020	6.5	-19.9	0.5	260.4	319.1	485.9	14.4
	FrucA2**	-4.490	6.613	11.103	4.5	-21.1		264.1	318.9	489.1	
	FrucA3**	-4.174	6.559	10.733	4.6	-20.8		265.7	318.7	488.0	
	FrucA4**	-4.325	6.416	10.741	5.5	-20.9		255.2	313.4	479.0	
	FrucA6**	-3.156	5.610	8.766	9.8	-19.3		259.5	319.7	484.1	
10	[F5-H]										
	F5A33***	-4.929	3.285	8.214	13.6	-61.8	-2.8	705.2	898.6	1787.1	68.1
	F5A34***	-5.021	3.306	8.327	16.5	-61.3		705.7	896.2	1790.6	
	F5A36***	-4.807	3.099	7.906	18.6	-58.4		677.9	895.1	1782.8	
	F5A16***	-5.229	3.324	8.553	11.4	-61.8		670.9	873.2	1744.9	
	F5A12***	-4.417	2.752	7.169	22.9	-61.8		709.1	901.4	1788.9	
	F5A13***	-4.425	2.887	7.312	19.4	-60.3		688.9	895.0	1782.7	
	F5A53***	-5.702	3.371	9.073	6.9	-61.7		678.9	890.9	1769.4	
11	[M5-H]										
	M5A32***	-4.014	3.143	7.157	7.6	-68.2		801.9	1020.5	1904.4	68.1
	M5A33***	-4.741	3.080	7.821	9.9	-67.8		773.6	1010.9	1897.8	
	M5A36***	-4.397	2.975	7.372	14.5	-65.4		768.1	1017.9	1889.5	
	M5A11***	-4.239	2.366	6.505	47.5	-67.1		795.7	1019.9	1903.5	
	M5A12***	-4.326	2.267	6.593	46.9	-67.0		769.1	1017.0	1885.9	
12	[M6-H]										
	M6A32***	-4.800	2.495	7.295	24.7	-78.9	-6.0	915.6	1194.7	2257.6	81.5
	M6A33***	-4.649	2.468	7.117	22.4	-79.6		910.6	1195.3	2251.5	
	M6A36***	-3.972	2.687	6.659	14.6	-78.7		917.9	1199.4	2246.9	
	M6A11***	-4.183	2.082	6.265	55.1	-78.8		926.5	1198.3	2251.8	
	M6A12***	-4.839	2.211	7.050	46.7	-77.3		884.5	1172.1	2224.2	
	M6A16***	-3.423	2.111	5.534	53.6	-78.8		925.1	1196.1	2249.8	
13	[M7-H]										
	M7A42***	-4.123	2.633	6.756	13.1	-89.2	-6.9	1086.1	1374.3	2611.9	99.3
	M7A46***	-4.138	2.793	6.931	12.2	-86.9		1057.9	1362.8	2594.4	
	M7A11***	-4.473	2.419	6.892	43.8	-87.5		1066.4	1361.4	2601.5	
14	[βCD-H]										
	bCDA2**	-5.854	2.929	8.783	15.0	-74.2	-6.8	833.7	1132.2	2377.9	93.5
	bCDA6**	-4.542	2.655	7.197	19.5	-75.0		886.1	1146.7	2378.3	

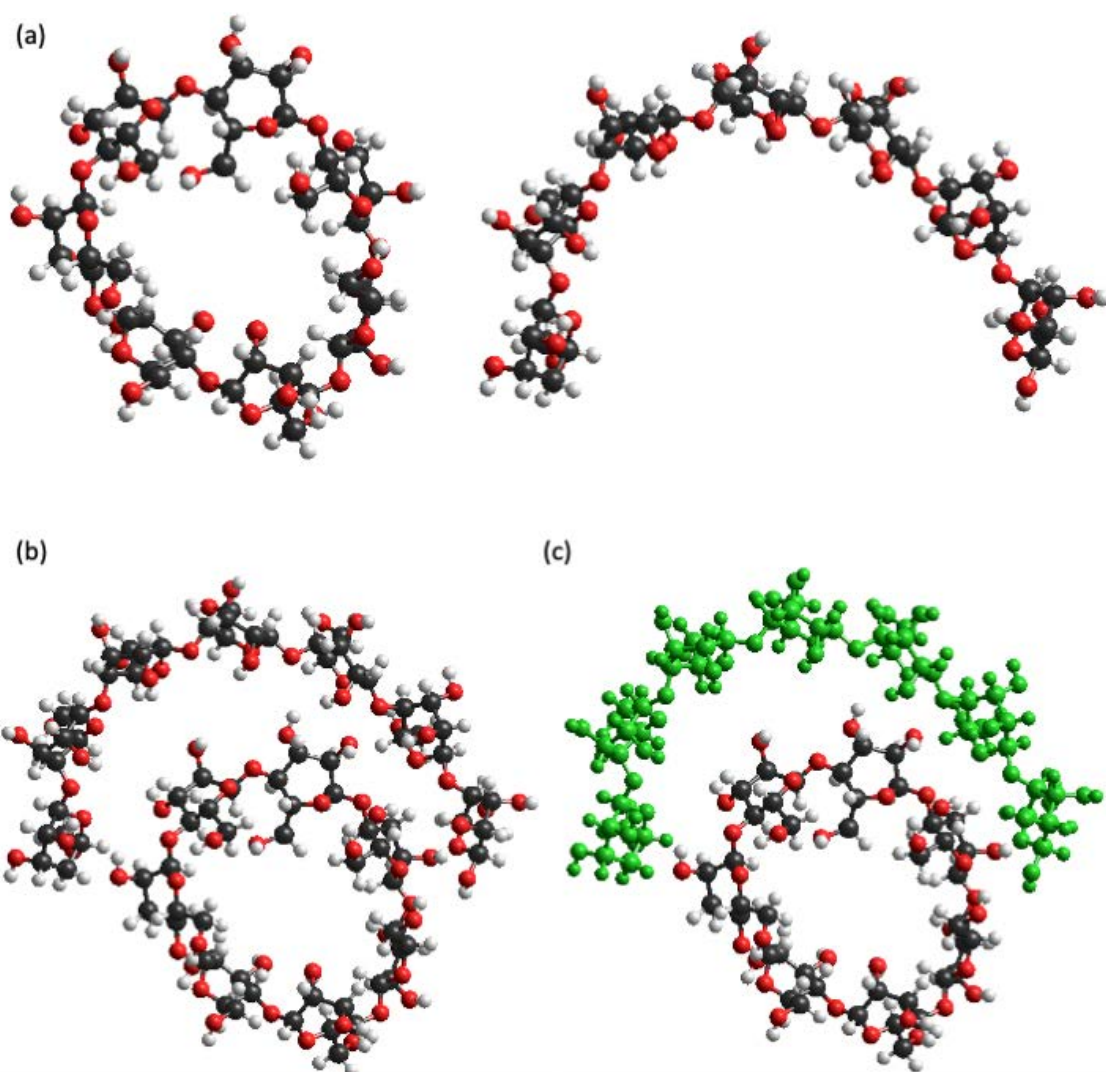
* Δ =LUMO-HOMO. **CarbAz: z is the molecule position of the C-OH group whose H is removed. *** CarbAxz: x is the molecule position of the monosaccharide moiety in the total Carb molecule structure; z is the position in the monosaccharide moiety of the C-OH group whose H is removed.



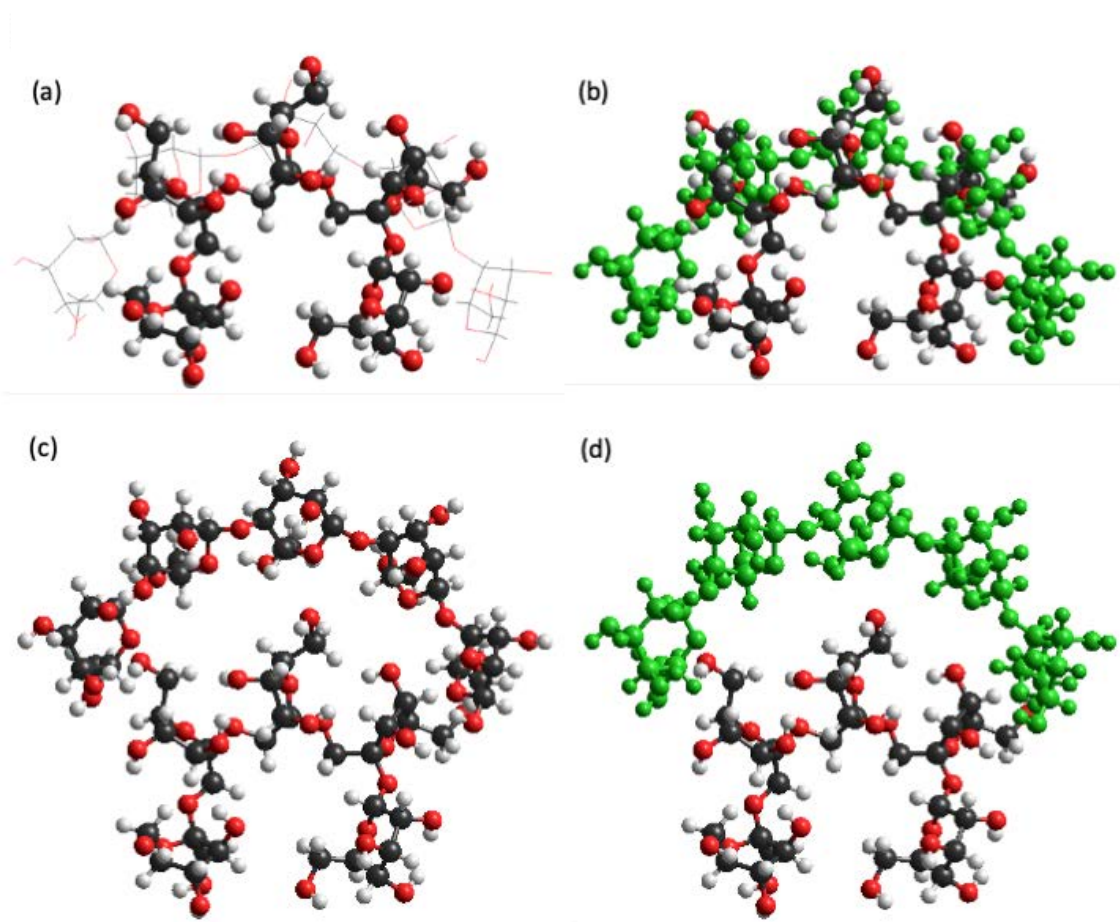
Scheme S1. (A) Additional details for Scheme 2 (c) included in main text: (left) ESA+Glc 1:1 complex. Glc in green except the two H atoms involved in the H bridges between ESA and Glc; (right) enhances view of the H bridges interaction region.



Scheme S1. (B) Optimized molecule geometry comparison for Glc (left) and Frc (right). Molecule views from two different planes (upper row, view from ceiling plane; bottom row, view from plane perpendicular to ceiling).

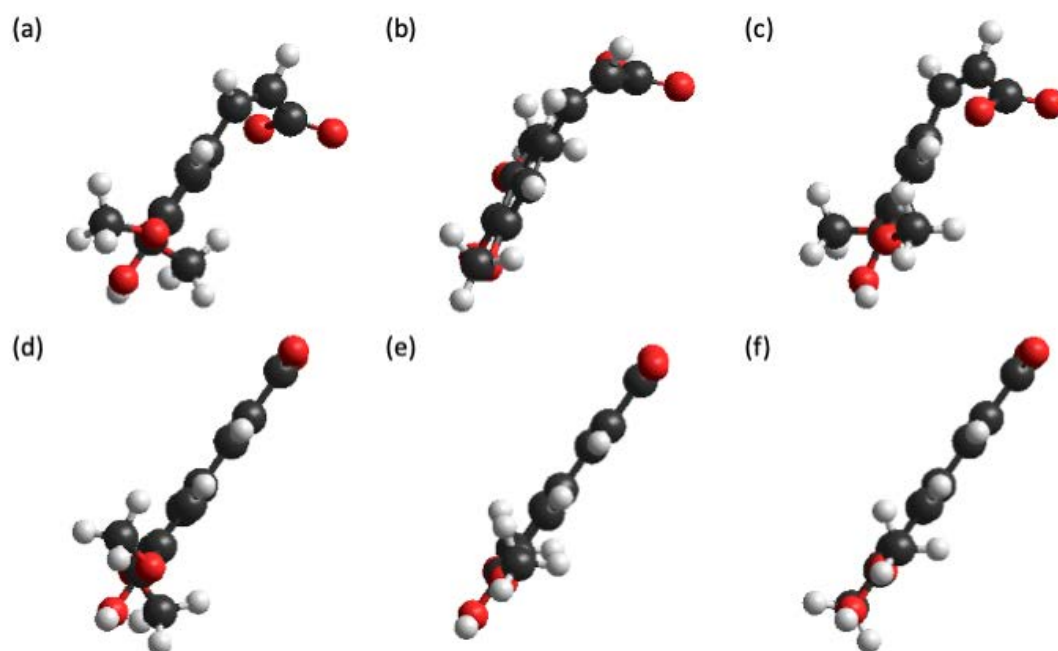


Scheme S1. (C) Optimized molecule geometry comparison for β CD and M7. (a) β CD (left) and M7 (right); (b) M7 (top) and β CD (bottom); (c) idem (b) with M7 in green.

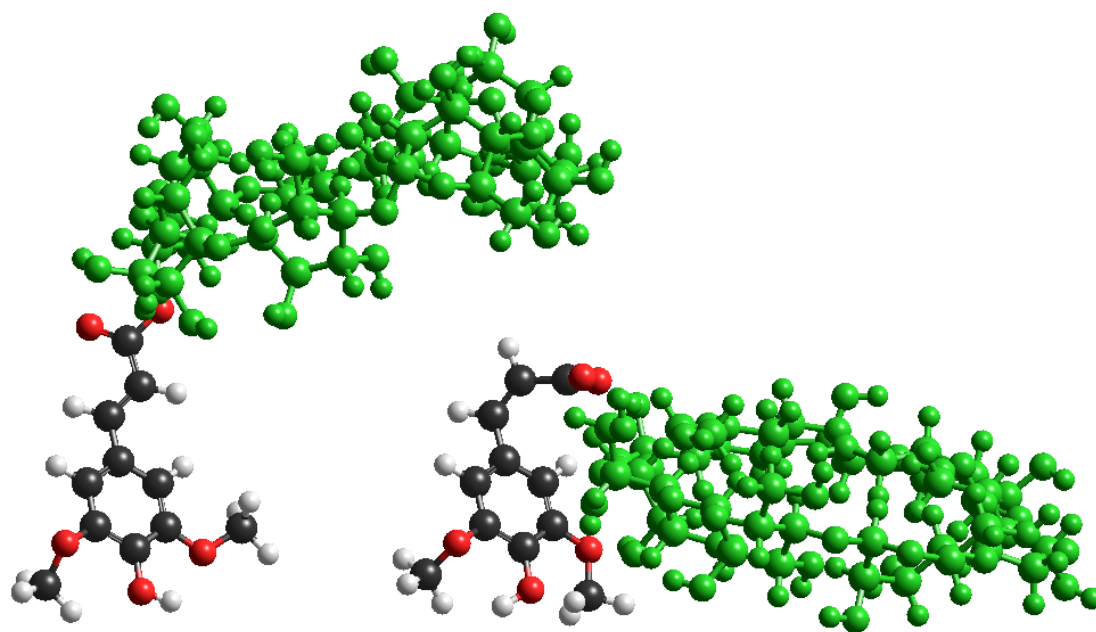


Scheme S1. (D) Optimized molecule geometry comparison for F5 and M5: (a) Artificial in silico superposition of molecules F5 (sticks and ball) and M5 (sticks); (b) Artificial in silico superposition of molecules F5 (sticks and ball) and M5 (sticks and balls in green); (c) M5 (top) and F5 (bottom) and (d) M5 (top) and F5, M5 in green.

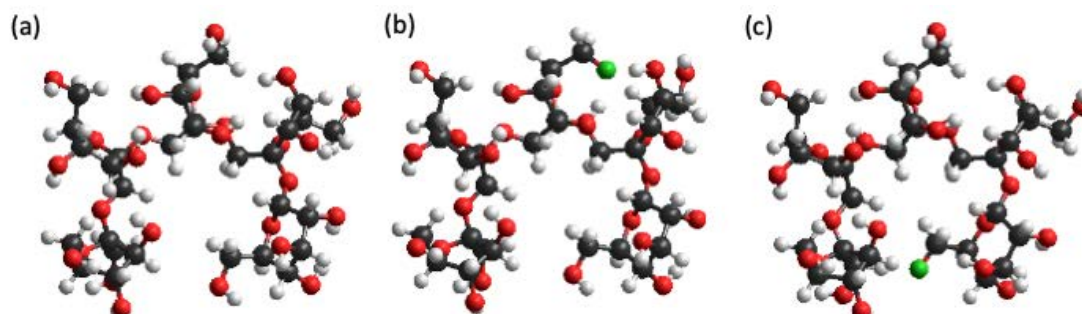
Scheme S1. (A) Additional details for Scheme 2 (c) included in main text: (left) ESA+Glc 1:1 complex. Glc in green except the two H atoms involved in the H bridges between ESA and Glc; (right) enhances view of the H bridges interaction region. (B) Optimized molecule geometry comparison for Glc (left) and Frc (right). Molecule views from two different planes (upper row, view from ceiling plane; bottom row, view from plane perpendicular to ceiling). (C) Optimized molecule geometry comparison for β CD and M7. (a) β CD (left) and M7 (right); (b) M7 (top) and β CD (bottom); (c) idem (b) with M7 in green. (D) Optimized molecule geometry comparison for F5 and M5: (a) Artificial on silico superposition of molecules F5 (sticks and ball) and M5 (sticks); (b) Artificial on silico superposition of molecules F5 (sticks and ball) and M5 (sticks and balls in green); (c) M5 (top) and F5 (bottom) and (d) M5 (top) and F5, M5 in green.



Scheme S2. Optimized molecule geometry comparison for $[\text{ZSA-H}]^-$ (top) and $[\text{ESA-H}]^-$ (bottom) rotamers whose QSAR and HOMO properties are included in Table S1. Details according to nomenclature in Table S1: $[\text{ZSA-H}]^-$ (top), left to right: $[\text{ZSA-H}]^-$, $[\text{ZSAp-H}]^-$ and $[\text{ZSAps-H}]^-$; $[\text{ESA-H}]^-$ (bottom), left to right: $[\text{ESA-H}]^-$, $[\text{ESAp-H}]^-$ and $[\text{ESAps-H}]^-$.



Scheme S3. Optimized molecule geometry comparison for [ESA-H]⁻ (left) and [ZSA-H]⁻ (right) complexes with βCD, [ESA+βCD-H]⁻ and [ZSA+βCD-H]⁻. βCD in green.



Scheme S4. Optimized molecule geometry comparison for F5 (a) and $[F5-H]^-$ (b and c), whose QSAR and HOMO properties are included in Table S2. Details according to nomenclature in Table S2: F5 (neutral molecule, a), $[F5-H]^-$ (anion in general): F5A36 (b), F5A16 (c). In the anionic species the deprotonated oxygen is indicated in green. The distortion of the molecule geometry allows a special stabilization because of the hydrogen bond formed involving this oxo-ion and a proton belonging to an HO group spatially located nearby, at an atom-atom distance $< 2 \text{ \AA}$ (Angstrom).

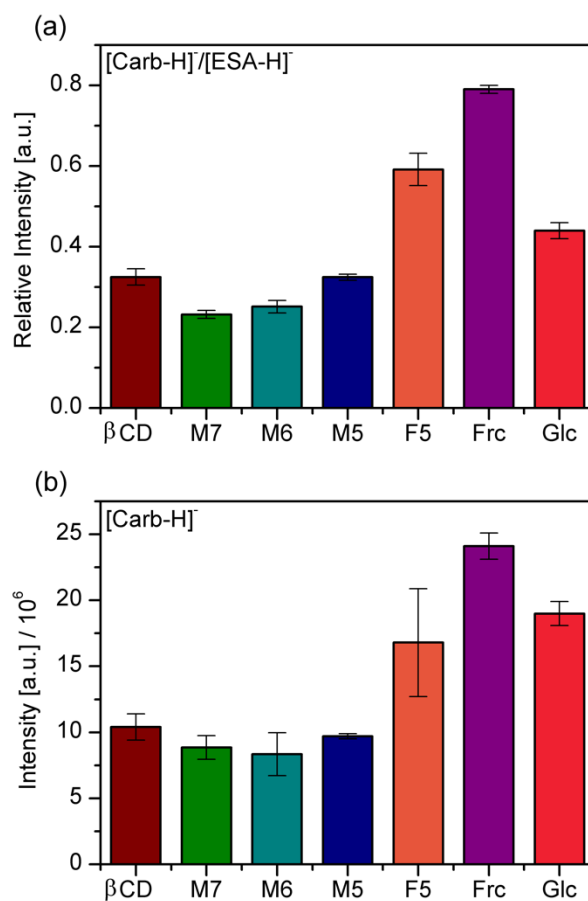


Figure S1. (a) Intensity of [Carb-H]⁻ peak relative to [ESA-H]⁻ ($[\text{Carb-H}]^- / [\text{ESA-H}]^-$) and (b) absolute intensity of [Carb-H]⁻ peak for each Carb studied. Carb 15 μM and ESA 5 μM in water: MeOH 7:3. ESA used as external calibrant (reference).

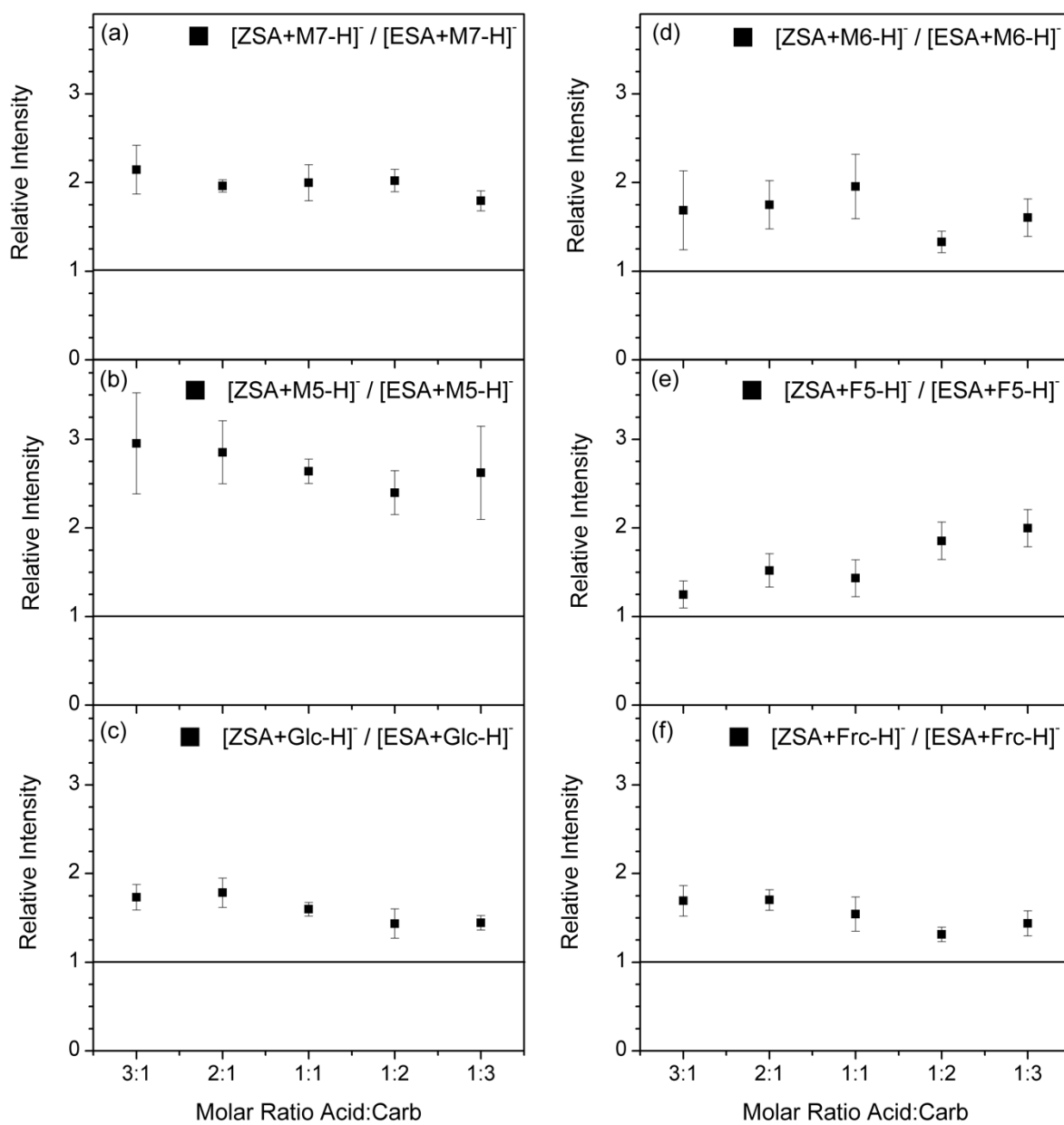


Figure S2. Intensity of the $[ZSA+Carb-H]^-$ peak relative to $[ESA+Carb-H]^-$, ($[ZSA+Carb-H]^- / [ESA+Carb-H]^-$), for different Acid:Carb molar ratios. Acid concentration 5 μM in all the experiments. Carbohydrate (Carb) studied: (a) M7, (b) M5, (c) Glc, (d) M6, (e) F5 and (f) Frc.

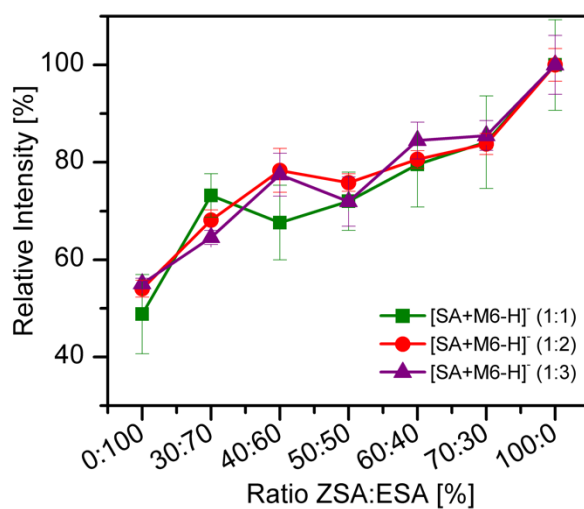
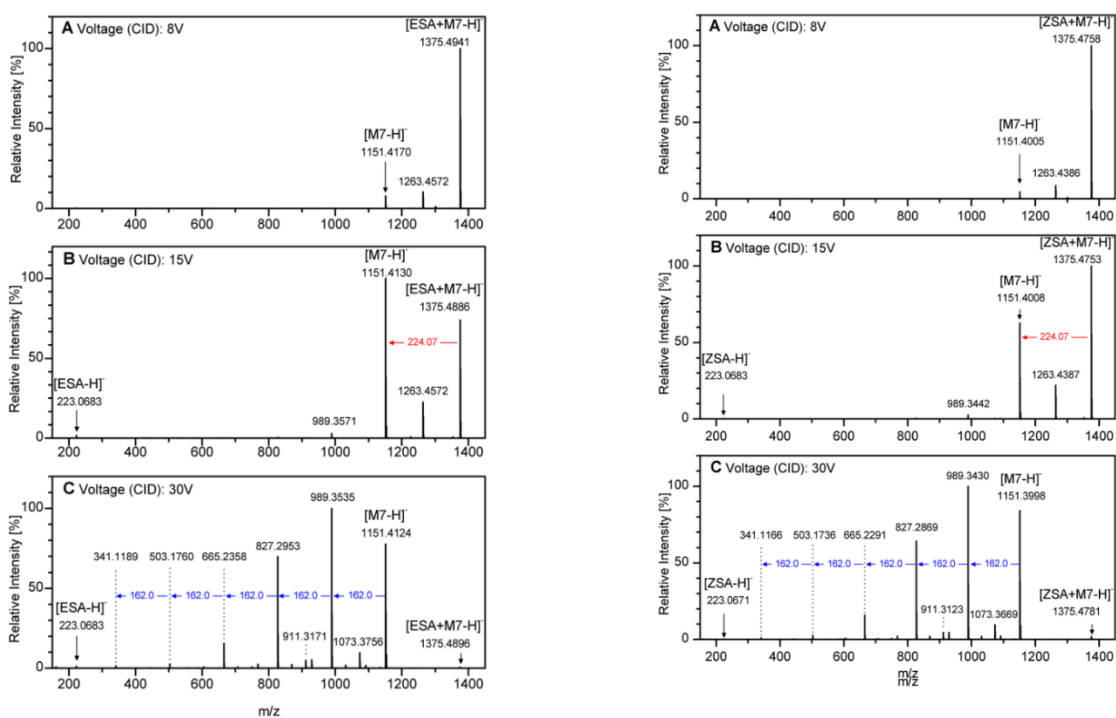
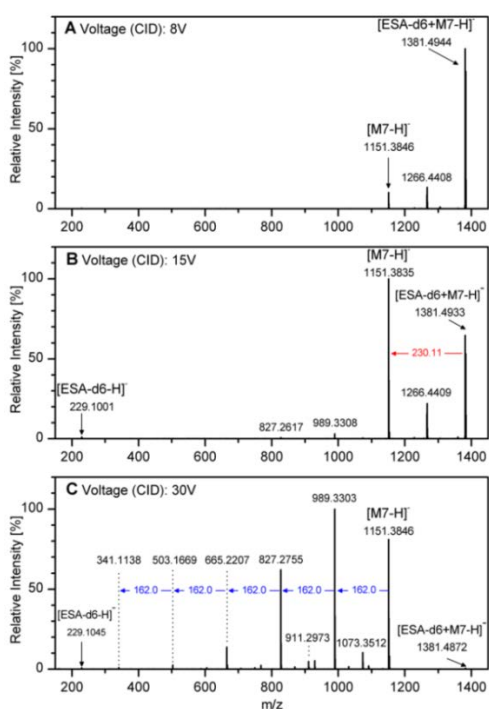


Figure S3. Competitive titration curves for Carb: M6. $[\text{Acid}+\text{M6-H}]^-$ peak intensity relative to $[\text{ZSA}+\text{M6-H}]^-$ peak intensity at ZSA:ESA 100:0%, ($[\text{Acid}+\text{M6-H}]^- / [\text{ZSA}+\text{M6-H}]^-$), vs ZSA:ESA % ratio. Acid:M6 (■) 1:1, (●) 1:2 y (▲) 1:3 mol/mol; Acid = ZSA+ESA from ZSA:ESA 0:100% to 100:0%.



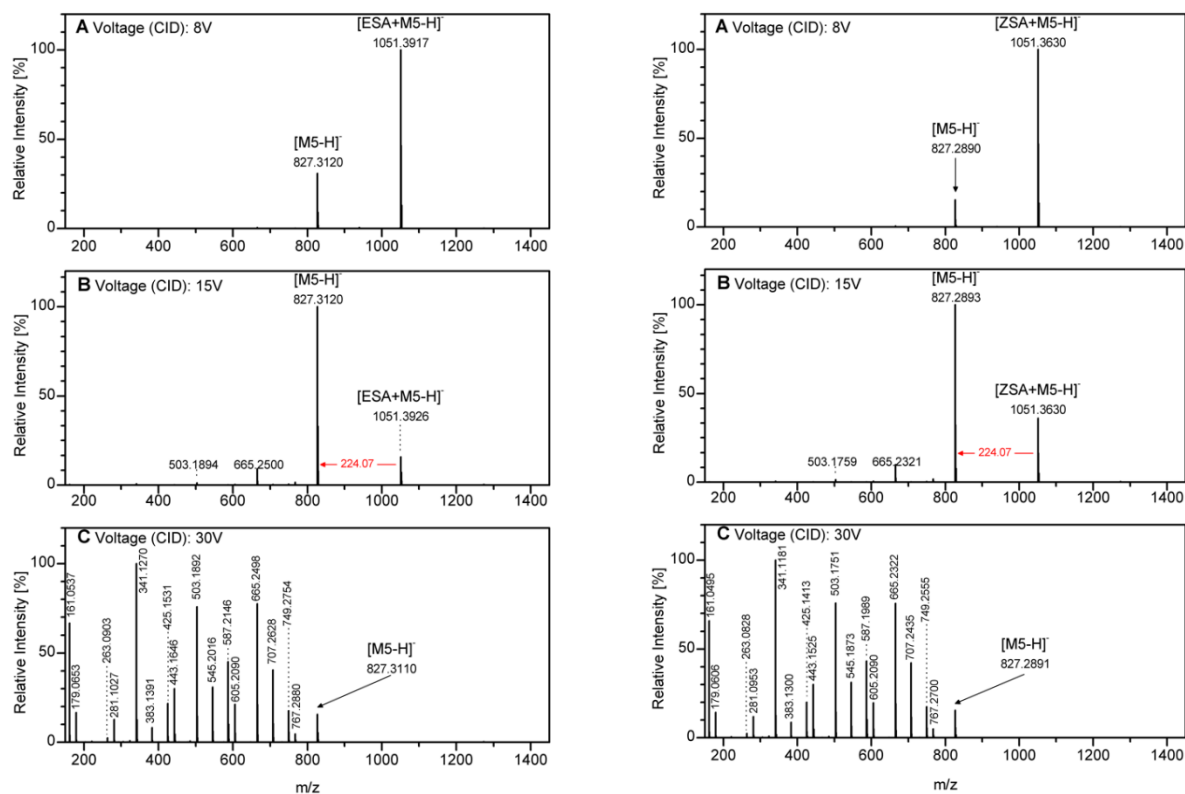
– MS/MS spectra. Precursor ion [ESA+M7-H]⁻. CID voltage, 8V (A), 15V (B) and 30V (C).

– MS/MS spectra. Precursor ion [ZSA+M7-H]⁻. CID voltage, 8V (A), 15V (B) and 30V (C).



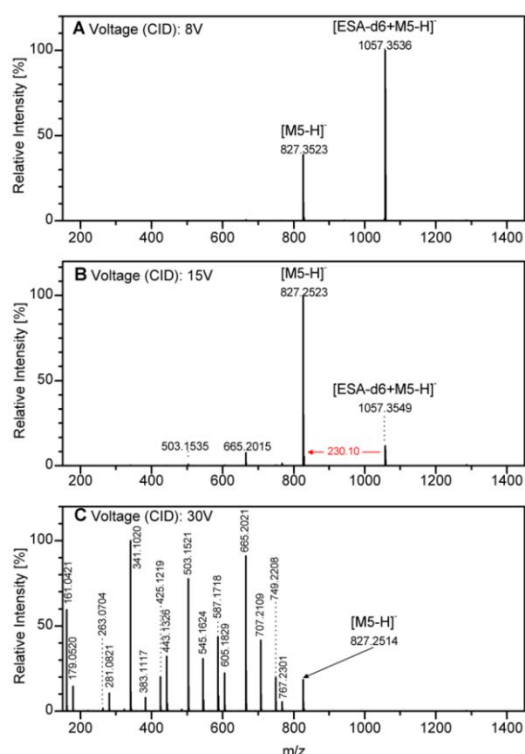
– MS/MS spectra. Precursor ion [ESA-d6+M7-H]⁻. CID voltage, 8V (A), 15V (B) and 30V (C).

Figure S4. MS/MS spectra. Precursor ions: [ESA+M7-H]⁻ (top, left), [ZSA+M7-H]⁻ (top, right) and [ESA-d6+M7-H]⁻ (bottom, left). CID voltage, 8V, 15V and 30V. Acid:M7 1:3 mol/mol; water:MeOH 7:3.



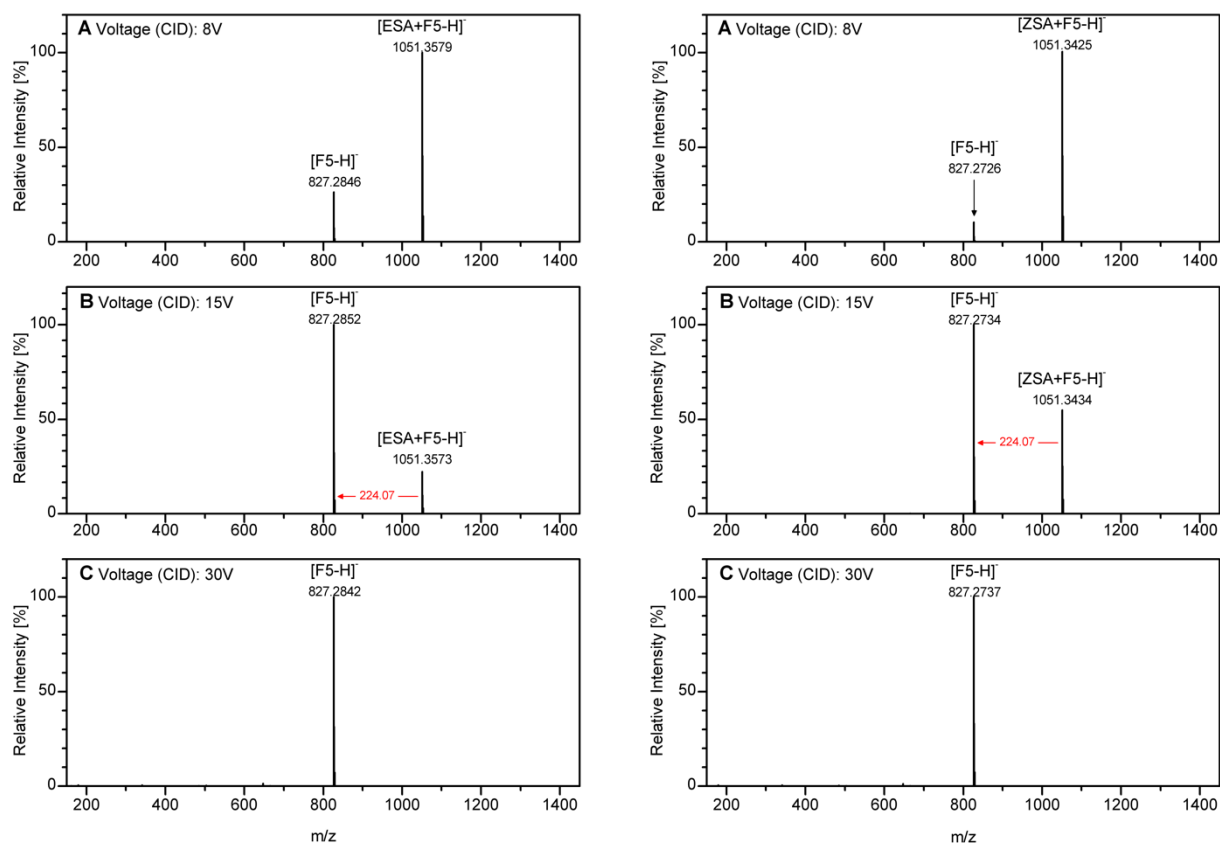
– MS/MS spectra. Precursor ion $[ESA+M5-H]^-$. CID voltage, 8V (A), 15V (B) and 30V (C).

– MS/MS spectra. Precursor ion $[ZSA+M5-H]^-$. CID voltage, 8V (A), 15V (B) and 30V (C).



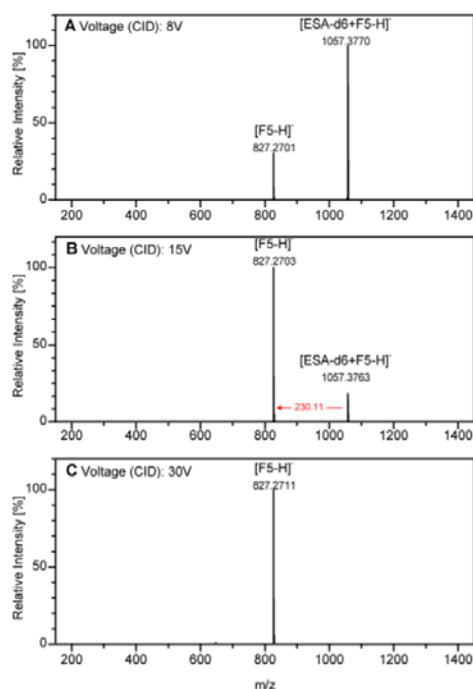
– MS/MS spectra. Precursor ion $[ESA-d6+M5-H]^-$. CID voltage, 8V (A), 15V (B) and 30V (C).

Figure S5. MS/MS spectra. Precursor ions: $[ESA+M5-H]^-$ (top, left), $[ZSA+M5-H]^-$ (top, right) and $[ESA-d6+M5-H]^-$ (bottom, left). CID voltage, 8V, 15V and 30V. Acid:M5 1:3 mol/mol; water:MeOH 7:3.



– MS/MS spectra. Precursor ion [ESA+F5-H]⁻. CID voltage, 8V (A), 15V (B) and 30V (C).

– MS/MS spectra. Precursor ion [ZSA+F5-H]⁻. CID voltage, 8V (A), 15V (B) and 30V (C).



– MS/MS spectra. Precursor ion [ESA-d6+F5-H]⁻. CID voltage, 8V (A), 15V (B) and 30V (C).

Figure S6. MS/MS spectra. Precursor ions: [ESA+F5-H]⁻ (top, left), [ZSA+F5-H]⁻ (top, right) and [ESA-d6+F5-H]⁻ (bottom, left). CID voltage, 8V, 15V and 30V. Acid:F5 1:3 mol/mol; water:MeOH 7:3.

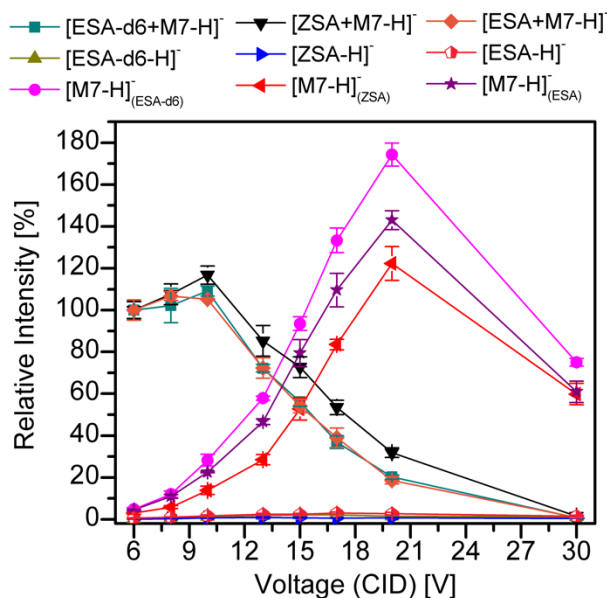


Figure S7. MS/MS (CID) experiments. Intensity of the species [Acid+M7-H]⁻, [Acid-H]⁻ and [M7-H]⁻ detected at different voltages relative to the value obtained at the lowest voltage (6V), Precursor ions [ESA-d6+M7-H]⁻ (■), [ESA+M7-H]⁻ (◆) and [ZSA+M7-H]⁻ (▼). Acid:M7 1:3 mol/mol; water:MeOH 7:3.

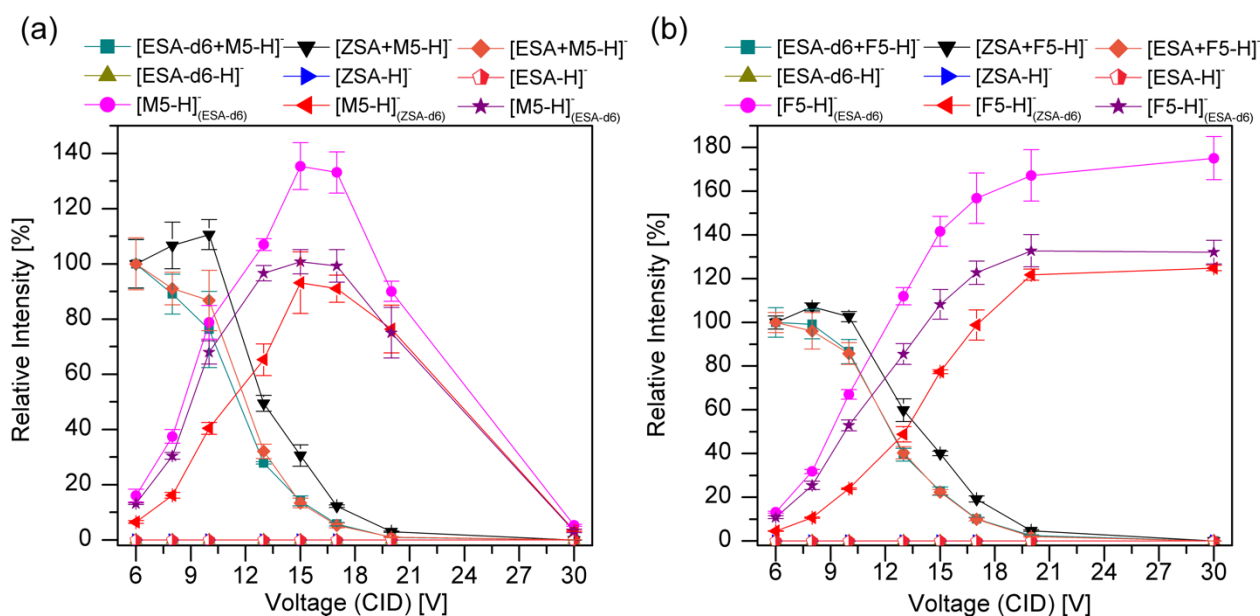


Figure S8. MS/MS (CID) experiments. Intensity of the species [Acid+Carb-H]⁻, [Acid-H]⁻ and [Carb-H]⁻ detected at different voltages relative to the value obtained at the lowest voltage (6V), Precursor ions: (a) left [ESA-d6+M5-H]⁻ (■), [ESA+M5-H]⁻ (◆) and [ZSA+M5-H]⁻ (▼); (b) right [ESA-d6+F5-H]⁻ (■), [ESA+F5-H]⁻ (◆) and [ZSA+F5-H]⁻ (▼). Acid:Carb 1:3 mol/mol; water:MeOH 7:3.

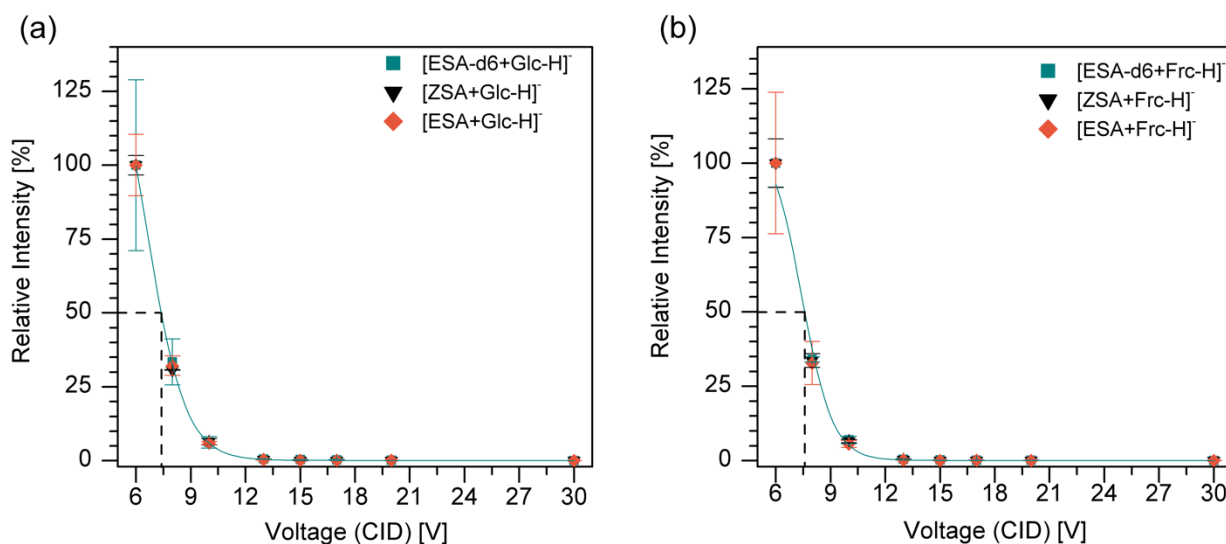


Figure S9. MS/MS (CID) experiments. Intensity of the species [Acid+Carb-H]⁻ detected at different voltages relative to the value obtained at the lowest voltage (6V), fitted curves. Precursor ions: (i) left [ESA-d6+Glc-H]⁻ (■), [ESA+Glc-H]⁻ (◆) and [ZSA+Glc-H]⁻ (▼); (ii) right [ESA-d6+Frc-H]⁻ (■), [ESA+Frc-H]⁻ (◆) and [ZSA+Frc-H]⁻ (▼). Acid:Carb 1:3 mol/mol; water:MeOH 7:3.

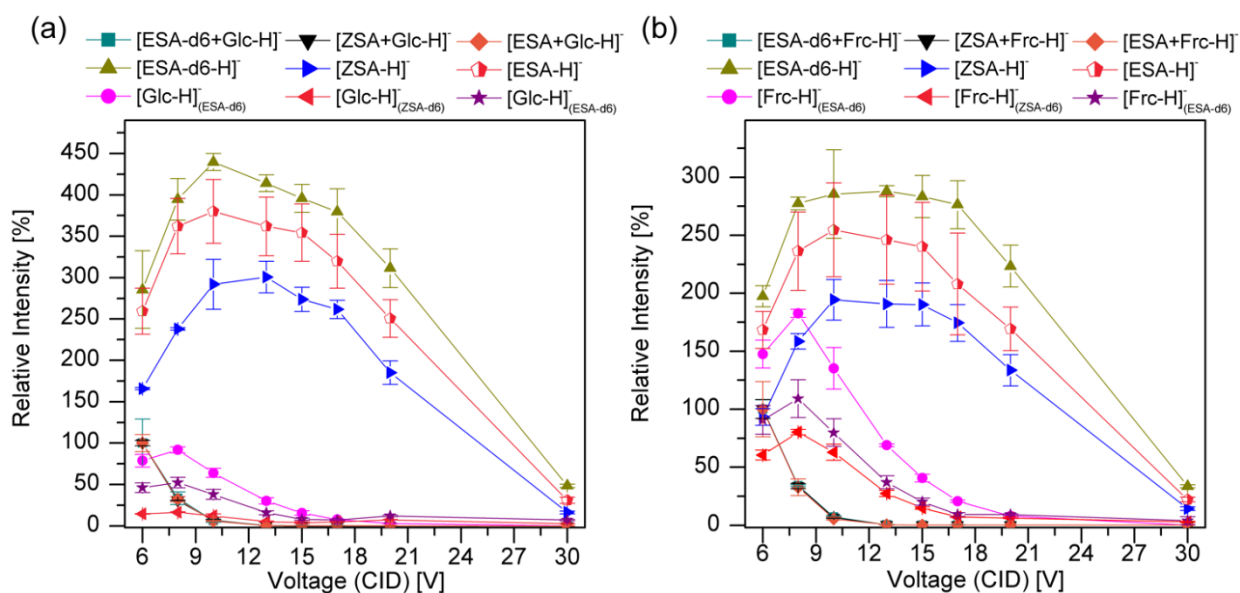


Figure S10. MS/MS (CID) experiments. Intensity of the species [Acid+Carb-H]⁻, [Acid-H]⁻ and [Carb-H]⁻ detected at different voltages relative to the value obtained at the lowest voltage (6V), Precursor ions: (i) left [ESA-d6+Glc-H]⁻ (■), [ESA+Glc-H]⁻ (◆) and [ZSA+Glc-H]⁻ (▼); (ii) right [ESA-d6+Frc-H]⁻ (■), [ESA+Frc-H]⁻ (◆) and [ZSA+Frc-H]⁻ (▼); Acid:Carb 1:3 mol/mol; water:MeOH 7:3.